Breakdown in Millimeter-Wave Power InP HEMT's: A Comparison with GaAs PHEMT's

J. A. del Alamo and M. H. Somerville

Abstract— **In spite of their outstanding transport characteristics, InP high-electron mobility transistors (HEMT's) deliver lower output power than GaAs pseudomorphic HEMT's (PHEMT's) throughout most of the millimeter-wave regime. However, the superior power-added efficiency of InP HEMT's when compared with GaAs PHEMT's makes this technology attractive for many applications. The reason for the relatively inferior power output of InP HEMT's lies in their comparatively small off-state and on-state breakdown voltages. This paper reviews the state of knowledge regarding the physics of breakdown voltage in InP HEMT's, placing it in contrast with GaAs PHEMT's. It also presents current understanding regarding burnout, a closely related phenomenon. This paper concludes by discussing strategies for improving the breakdown voltage and the power output of InP HEMT's.**

Index Terms— **Breakdown voltage, high electron mobility transistor (HEMT), InGaAs, power, pseudomorphic HEMT (PHEMT).**

I. INTRODUCTION

THE use of InAlAs/InGaAs high-electron mobility transistors (HEMT's) on InP (or InP HEMT's, for short) in low-noise applications is well established. Their suitability for millimeter-wave power amplification is still a matter of debate. At this time, a review of the literature shows that GaAs pseudomorphic HEMT's (PHEMT's) exhibit higher power output than InP HEMT's across nearly the entire frequency spectrum from 1 to 100 GHz (Fig. 1). Only at 94 GHz and due to a recent report [1], InP HEMT's match the power level of GaAs PHEMT's [2], [3]. The data shown in Fig. 1 come from literature publications of devices and amplifiers of different designs operating at room temperature. Recent representative work from the various players can be found in [1]–[7].

Output power is not the only figure of merit with which millimeter-wave system designers are concerned. Power-added efficiency (PAE) is a critical concern in most systems. Fig. 2 graphs reported gain per stage and power-added efficiency versus output power for devices and amplifiers at 94 GHz. At all power levels above 20 mW or so, InP HEMT's exhibit substantially enhanced gain per stage than GaAs PHEMT's. As a result, the power-added efficiency of InP HEMT's exceeds that of GaAs PHEMT's by about ten percentage points across the entire power range. This makes InP power HEMT technology attractive for applications where large numbers of transmitters are integrated together in a small volume, such as phase-array radar, W-band imaging systems, and collision avoidance for automotive applications [8]–[10].

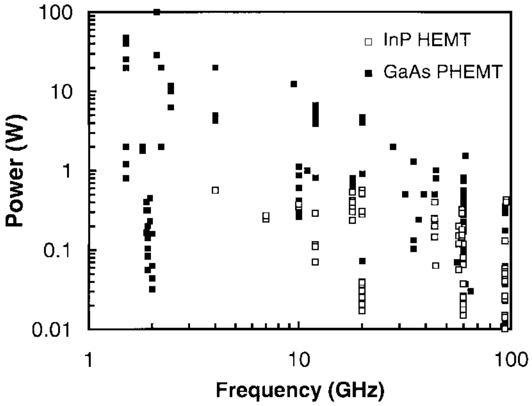

Fig. 1. Reported output power versus frequency for devices and power amplifiers based on InP HEMT's and GaAs PHEMT's.

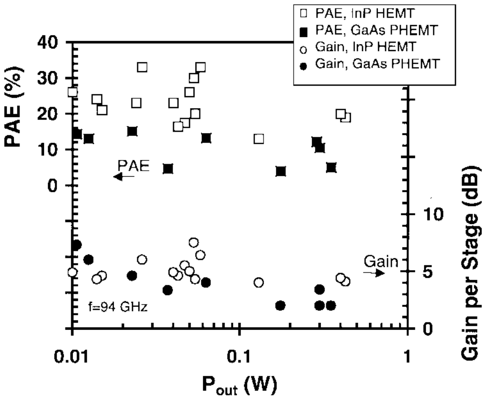

Fig. 2. Reported gain-per-stage and power-added efficiency for devices and power amplifiers based on InP HEMT and GaAs PHEMT at 94 GHz as a function of output power.

The reason for the relatively inferior power performance of InP HEMT's can be understood by examining the data shown in Fig. 3, which plots 94-GHz power density attained in InP HEMT and GaAs PHEMT power devices and amplifiers versus the drain-to-source bias used for the field-effect transistor (FET). This figure shows that the device bias selected in InP power HEMT's is on average about 1 V lower than in GaAs PHEMT's. This stems from two facts that will be extensively discussed in this paper.

Manuscript received February 8, 1999; revised April 2, 1999. This work was supported by JSEP, MAFET, Lockheed Martin Sanders, HP, NTT, TI, and NSF.

J. A. del Alamo is with the Massachusetts Institute of Technology, Cambridge, MA 02139 USA.

M. H. Somerville was with the Massachusetts Institute of Technology, Cambridge, MA 02139 USA. He is now with Vassar College, Poughkeepsie, NY 12601 USA.

Publisher Item Identifier S 0018-9200(99)06479-3.

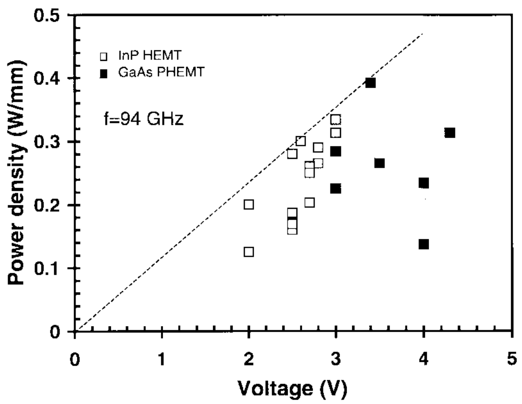

Fig. 3. Reported power density for devices and power amplifiers based on InP HEMT's and GaAs PHEMT's at 94 GHz as a function of the drain-to-source bias voltage selected for the transistor.

1) For a given maximum current, InP HEMT's exhibit an *off-state* breakdown voltage ($BV_{\rm off}$) about 2–3-V lower than GaAs PHEMT's.
2) For a given $BV_{\rm off}$, InP HEMT's have significantly worse *on-state* breakdown voltage ($BV_{\rm on}$) than GaAs PHEMT's.

Fig. 3 also shows that at an equal bias voltage, InP HEMT's match or exceed the power density of GaAs PHEMT's. This stems from the higher current drivability of InP HEMT's. In consequence, if the breakdown voltage of InP HEMT's could be enhanced without significantly affecting the overall performance of the device, InP HEMT's might exceed the power output of GaAs PHEMT's.

This paper reviews the state of knowledge of breakdown in InP and GaAs millimeter-wave power HEMT's. It is organized as follows. Section II discusses issues relevant to the definition and measurement of the breakdown voltage. Section III reviews current understanding of the physics of breakdown voltage in InP HEMT's and puts it in contrast with GaAs PHEMT's. A closely related phenomenon, burnout, is also discussed. Section IV argues that $BV_{\rm on}$ rather than $BV_{\rm off}$ is the bottleneck limiting the power output of InP HEMT's. This section then examines options for breakdown voltage improvement in InP HEMT's.

II. BREAKDOWN VOLTAGE CHARACTERIZATION

Understanding the physics of the breakdown voltage of HEMT's in general, and InP HEMT's in particular, has been hampered by three problems: the definition of breakdown voltage, its measurement, and the difficulty in obtaining systematic measurements of breakdown voltage on a single device. These difficulties have been recently resolved through the introduction of new characterization techniques that establish an unambiguous definition for the breakdown voltage. These new techniques are simple and relatively safe for the device. As a result, they can be performed repeatedly under different conditions (such as temperature) on the same device.

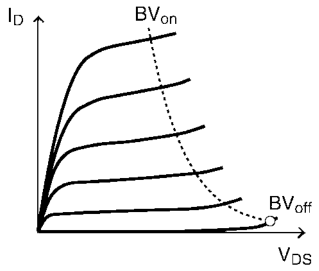

Fig. 4. Cartoon of output characteristics of typical HEMT depicting the off-state and on-state breakdown voltages. While $BV_{\rm off}$ refers to a point at or close to threshold, $BV_{\rm on}$ is a locus in the I_D–$V_{\rm DS}$ characteristics.

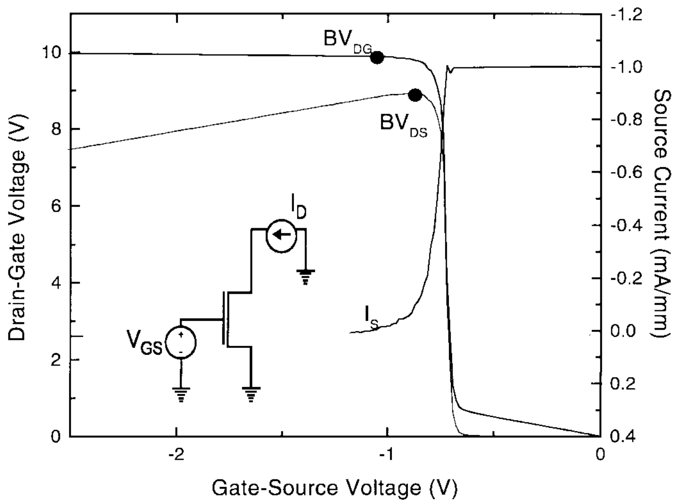

Fig. 5. Illustration of *drain-current injection technique* to measure $BV_{\rm off}$ in a typical InP HEMT. The inset shows the measurement scheme.

When discussing breakdown voltage, it is important to distinguish between *off-state* and *on-state* breakdown voltage. As the cartoon in Fig. 4 shows, off-state breakdown voltage refers to the maximum drain-to-source (or drain-to-gate) voltage that can be applied with the device in the *off* condition, that is, at or below threshold. A gate current of 1 mA/mm is commonly selected as the condition that defines the off-state breakdown voltage. How far below threshold the device is biased is one ambiguity that complicates this traditional definition.

In 1993, the *drain-current injection technique* was introduced to measure $BV_{\rm off}$ [11]. The measuring configuration and a typical result are shown in Fig. 5. This is a three-terminal technique that defines drain-to-gate off-state breakdown as the condition that results in $-I_G = I_D$ with the device in cutoff for a predetermined current criteria, typically, $I_D = 1$ mA/mm [11]. Drain-to-source off-state breakdown is defined as the maximum value of $V_{\rm DS}$ that can be obtained for a certain I_D criteria, typically $I_D = 1$ mA/mm. In these definitions, there is no ambiguity in the selection of the gate-source voltage. As a result, these definitions enable the automatic extraction of $BV_{\rm DG,off}$ and $BV_{\rm DS,off}$ [11]. In well-behaved devices, as shown in Fig. 5, the values of $V_{\rm GS}$ that correspond to each breakdown voltage are usually very close. Typically, the condition $I_G = -I_D$ for current levels around 1 mA/mm is obtained right below threshold, as in the example of Fig. 5. Since the device is biased with a current source at the drain, it is in a very safe state, and multiple measurements are possible.

The on-state breakdown voltage is usually defined as the *locus* in the I_D–$V_{\rm DS}$ characteristics for $V_{\rm GS}$ above threshold

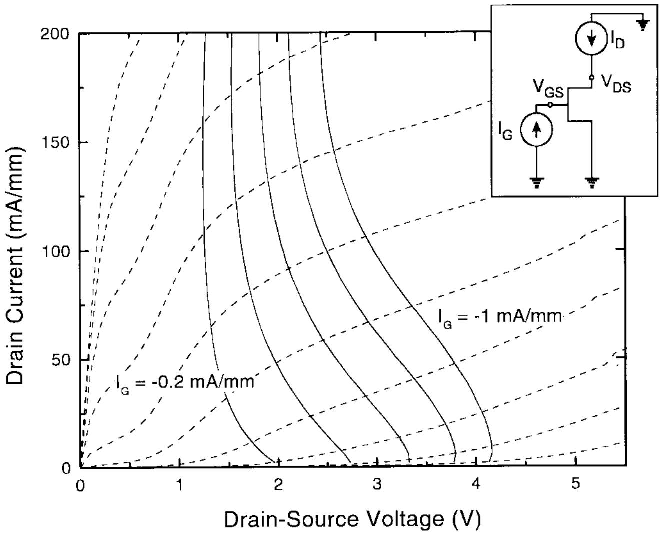

Fig. 6. Illustration of *gate-current extraction technique* to measure $BV_{\rm on}$ in a typical InP HEMT. The locus of constant I_G overlaps the output characteristics of the device (these look unusual in this figure due to the fact that the top of the scale on the y-axis is only 200 mA/mm). The inset shows the measurement scheme.

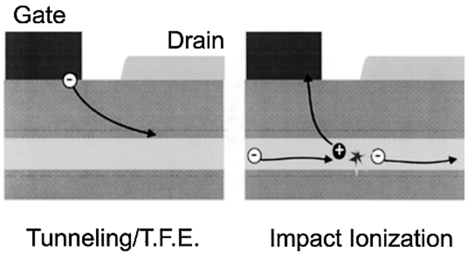

Fig. 7. Schematic diagram of thermionic-field emission and impact ionization in power HEMT's. These are the dominant breakdown mechanisms for $BV_{\rm off}$ and $BV_{\rm on}$, respectively, in both GaAs PHEMT's and InP HEMT's.

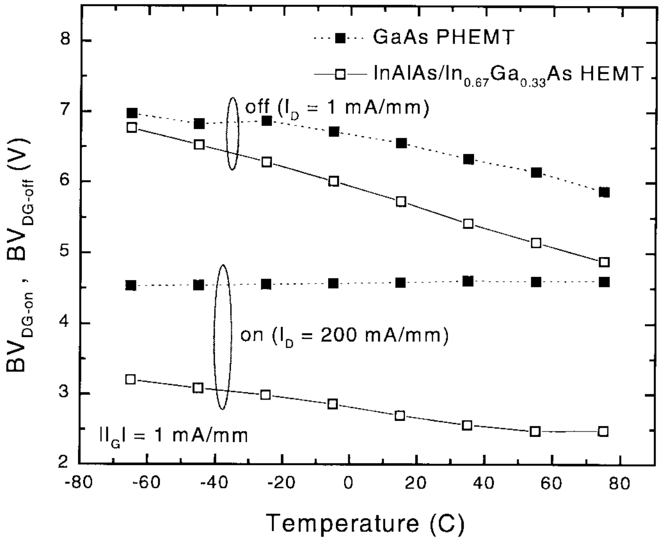

Fig. 8. Temperature dependence of $BV_{\rm off}$ and $BV_{\rm on}$ in a 0.1-μm GaAs power PHEMT and a 0.1-μm strained-channel power InP HEMT.

that meet a certain criteria (see cartoon in Fig. 4). Several such criteria have been proposed, yielding a great deal of ambiguity to the proper definition and measurement of $BV_{\rm on}$ [12].

In 1998, the *gate-current extraction technique* was introduced to measure $BV_{\rm on}$ [13]. This is also a three-terminal technique that defines breakdown as a *locus of constant gate current*, typically $I_G = -1$ mA/mm. As discussed later in this paper, this definition makes good physical sense. When the device is biased sufficiently above threshold, the gate current maps fairly accurately the impact ionization current generated in the device [12]. As shown in the inset of Fig. 6, the gate-current extraction technique biases the device by means of current sources and therefore maintains it in a rather safe state. Multiple measurements of the same device under different conditions are possible. A typical result is shown in Fig. 6 where an InP HEMT was biased at several values of I_G while I_D was ramped from $-I_G$ to 200 mA/mm [13]. In Fig. 6, the resulting I_D–$V_{\rm DS}$ breakdown loci (solid lines) are shown overlapped to the output characteristics (dashed lines). The I_D–$V_{\rm DS}$ loci have the shape that is to be expected for $BV_{\rm on}$. A satisfying feature of this pair of characterization techniques is that $BV_{\rm on}$ converges to $BV_{\rm off}$ as the device is turned off.

III. PHYSICS OF BREAKDOWN

In the last few years, great progress has been made toward the understanding of the physics of breakdown in HEMT's [11]–[19]. As a result of this effort, we now know that in well-designed and manufactured devices, there are essentially two physical mechanisms that can dominate the physics of breakdown in HEMT's: 1) tunneling or thermionic-field emission (TFE) of gate electrons and 2) impact ionization (II) of channel electrons. Both mechanisms are sketched in Fig. 7.

In GaAs PHEMT's, it is possible to separate thermionic emission from impact ionization through the temperature dependence of the breakdown voltage. Fig. 8 shows an example. This figure graphs $BV_{\rm off}$ and $BV_{\rm on}$ for a 0.1-μm GaAs PHEMT and a 0.1-μm InP HEMT. $BV_{\rm off}$ for the GaAs PHEMT exhibits a negative temperature coefficient, suggesting that it is TFE dominated, while its $BV_{\rm on}$ has a small but positive temperature coefficient, indicating that is dominated by impact ionization.

For InP HEMT's, the situation is complicated by the fact that the temperature coefficient of impact ionization for $In_xGa_{1-x}As$ experiences a sign reversal at some point between $x = 0.25$ and $x = 0.53$ [17], [20]. This is a consequence of the narrow bandgap of InAs-rich InGaAs. Because of this, in InP HEMT's, both $BV_{\rm off}$ and $BV_{\rm on}$ exhibit a negative temperature coefficient. This is seen in the data graphed in Fig. 8. It is possible, however, to unambiguously determine the dominant mechanism responsible for breakdown in InP HEMT's by means of a sidegate test structure that monitors hole generation due to channel impact ionization [12]. A study of this kind has established that similarly to GaAs PHEMT's, $BV_{\rm off}$ in InP HEMT's is dominated by thermionic field emission of gate electrons while $BV_{\rm on}$ is dominated by impact ionization of channel electrons.

A simple physics-based model has been recently developed for $BV_{\rm off}$ [18], [21], [22]. This model exploits the high aspect ratio of the electrostatics of a "well-designed" power HEMT

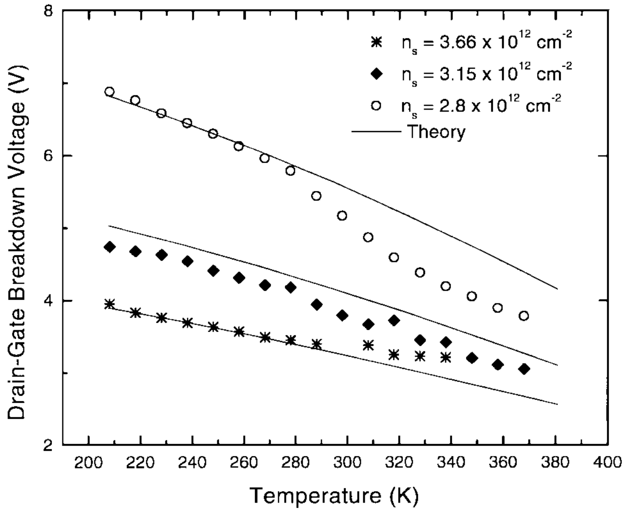

Fig. 9. Experimental and modeled $BV_{\rm off}$ versus temperature for 0.1-μm InP HEMT's with different values of channel sheet carrier concentration. The two inputs to the model, n_s and ϕ_B, are determined independently.

at breakdown to accurately model tunneling and TFE. A well-designed power device is one that features a relatively high breakdown voltage when compared with the threshold voltage. Due to the common use of a lightly doped or completely depleted caps, in a power HEMT at breakdown the depletion region on the drain side of the device exhibits a high aspect ratio: its extension in the direction of the drain is significantly larger than the channel thickness. Under these conditions, a simple conformal transform can be used to model the depletion region electrostatics [22], [23].

This model for $BV_{\rm off}$ has allowed the identification of the Schottky barrier height of the gate metal ϕ_B and the sheet carrier concentration in the extrinsic channel n_s as the two key parameters determining $BV_{\rm off}$. Such a simple model predicts well both the absolute value and also the temperature evolution of $BV_{\rm off}$ of InP power HEMT's. Fig. 9, for example, shows a comparison between measurements and simulations of $BV_{\rm off}$ in 0.1-μm InP power HEMT's [21]. In this comparison, both inputs to the model are obtained independently: ϕ_B from temperature-dependent measurements of the I–V characteristics of a gate diode and n_s through Hall measurements on capless structures. For a selectively gate recessed structure, this is the value of n_s that appears on the extrinsic drain right next to the gate and therefore is the one that largely determines the breakdown voltage.

Fig. 9 reveals that the agreement between theory and experiments is indeed good. Only in the sample with the lowest sheet carrier concentration some significant disagreement is found at high temperatures. In this regime, the predicted breakdown voltage is higher than the measured value. This is due to the appearance of substantial impact ionization even at the 1 mA/mm current level, as will become clear below. A refined model that incorporates a gate current contribution resulting from holes generated by impact-ionization, as discussed below, should correct this disagreement.

The proposed model for $BV_{\rm off}$ explains the superior values of $BV_{\rm off}$ observed in GaAs PHEMT's when compared with InP HEMT's. Fig. 10 shows a graph of reported values of $BV_{\rm off}$ for both types of devices as a function of the maximum drain current that flows through the device. For a given channel material, the maximum current is a rather reliable indicator of the extrinsic sheet carrier concentration on the drain side of the device. To make the comparison meaningful, all the devices captured in Fig. 10 have titanium as the bottom metal in the gate stack. For the same $I_{D\,\max}$, Fig. 10 reveals that on average GaAs PHEMT's feature a higher $BV_{\rm off}$ than InP HEMT's. The reason for this is the ~0.1-eV enhanced Schottky barrier height that is obtained on AlGaAs over In$_{0.52}$Al$_{0.48}$As [24]. Fig. 10 also includes two theoretical lines that have been calculated from our model. They represent reasonable upper limits to the best reported data in GaAs PHEMT's and InP HEMT's. They also indicate that a 0.1-eV difference in ϕ_B can result in a difference of several volts in $BV_{\rm off}$.

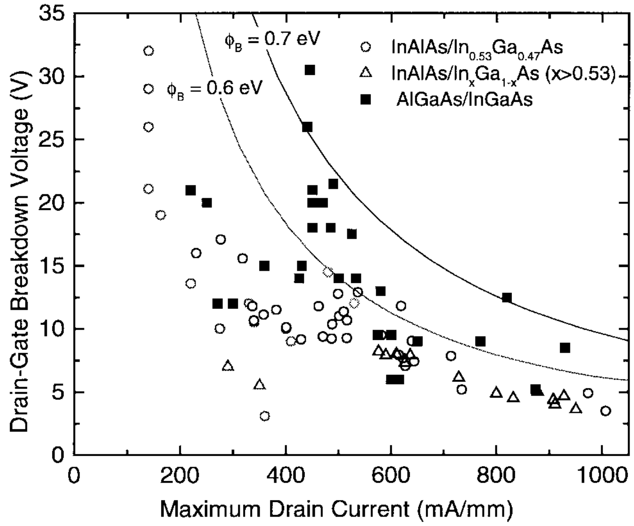

Fig. 10. Reported $BV_{\rm off}$ versus maximum drain current for InP HEMT's (lattice matched and pseudomorphic) and GaAs PHEMT's. In all these devices, Ti is the bottom metal of the gate stack. For the same $I_{D\,\max}$, GaAs PHEMT's exhibit a higher value of $BV_{\rm off}$ than InP HEMT's. There is no systematic difference in $BV_{\rm off}$ between lattice-matched and pseudomorphic InP HEMT's.

The model for $BV_{\rm off}$ further suggests that, contrary to conventional wisdom, the InAs composition of the channel of InP HEMT's should be of minor importance to $BV_{\rm off}$. The collection of data graphed in Fig. 10 indeed is consistent with this prediction. There is no systematic difference in $BV_{\rm off}$ between InP HEMT's with lattice-matched or InAs-rich strained channels. On first sight, this might appear contrary to some experiments with devices that only differ in the InAs composition in the channel [25]. It is commonly observed that the breakdown voltage degrades as the InAs composition is increased. The reason for this, however, is not the enhanced InAs composition but the higher channel sheet carrier concentration that results from the enlarged conduction band discontinuity between the channel and the gate insulator [26]. Once this is factored, as done in Fig. 10, the difference disappears.

While an entirely physics-based model of $BV_{\rm on}$ is yet to be developed, a simple phenomenological model for impact ionization coupled with the thermionic field emission model discussed above has been shown to give good agreement for

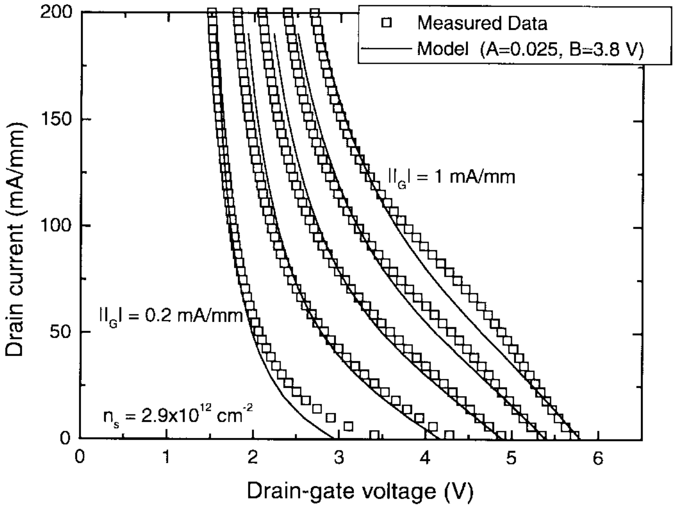

Fig. 11. Experimental and modeled $BV_{\rm on}$ contours in a 0.1-μm power InP power HEMT for different I_G criteria.

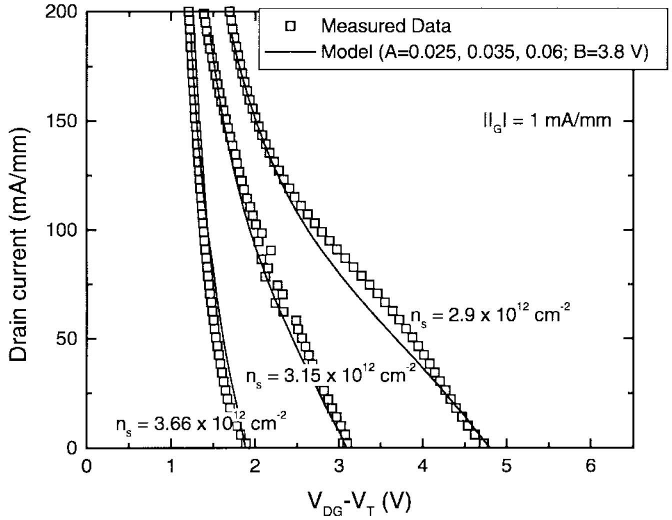

Fig. 12. Experimental and modeled $BV_{\rm on}$ contours for 0.1-μm power InP HEMT's with different values of sheet carrier concentration. Except for n_s, the devices are identical. They were all fabricated in the same run.

$BV_{\rm on}$ in InP HEMT's. Fig. 11 shows a comparison of the model against measurements for 0.1-μm InP power HEMT's at different gate current levels [12]. The model invokes a typical multiplication coefficient-type dependence for the gate current with two adjustable parameters [12]. One of these parameters establishes the dependence of the generation rate on the electric field on the drain and can be obtained independently from sidegate current measurements [12]. The second parameter is the proportionality constant between gate current and impact ionization rate and must be fit to the data. As Fig. 11 shows, the model matches very well the locus of $BV_{\rm on}$ for different values of I_G and I_D. Similarly, the model agrees well with $BV_{\rm on}$ for different devices with different values of sheet carrier concentration in the channel, as shown in Fig. 12. The good agreement shown in Figs. 11 and 12 gives us hope that an entirely physics-based model for $BV_{\rm on}$ is an attainable goal.

The $BV_{\rm on}$ model illuminates the shifting relative importance of impact ionization and thermionic field emission at breakdown as the device is turned on. This is understood best by examining the locus of $BV_{\rm on}$ for devices with different sheet carrier concentrations in the channel that is shown in Fig. 12. In devices with low values of sheet carrier concentration, $BV_{\rm off}$ is high and the field at $BV_{\rm off}$ is rather spread out on the drain. As a result, as the device is turned on, impact ionization increases quickly and $BV_{\rm on}$ degrades rapidly. In contrast, if the sheet carrier concentration is high, $BV_{\rm off}$ is small and the field on the drain is tightly confined. In consequence, when the device is turned on, impact ionization builds up gradually and the $BV_{\rm on}$ characteristics are rather vertical.

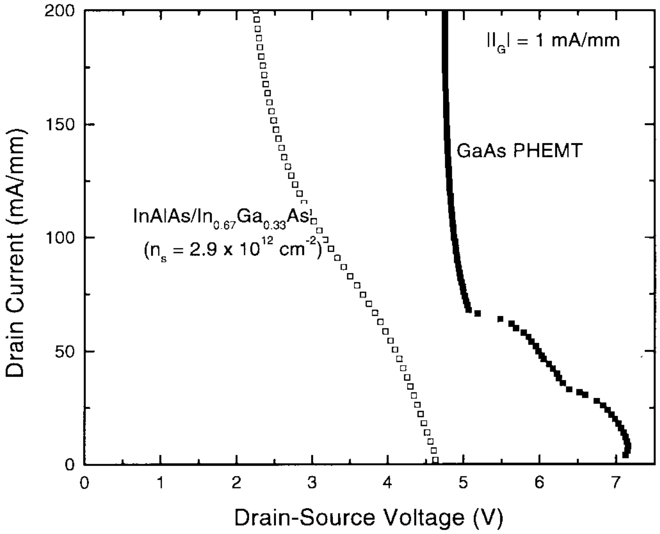

Fig. 13. $BV_{\rm on}$ for a 0.1-μm InP power HEMT and a 0.1-μm GaAs PHEMT. Both devices have a similar sheet carrier concentration. The erosion of $BV_{\rm on}$ is most severe in the case of the InP HEMT.

While a similar mechanism occurs in GaAs PHEMT's, the lower impact ionization rate in these devices results in a comparatively less severe breakdown voltage degradation when the device is turned on. This is clearly seen in Fig. 13 where the $BV_{\rm on}$ locus of a 0.1-μm InP HEMT and a 0.1-μm GaAs PHEMT with similar sheet carrier concentrations are shown. Due to the higher Schottky barrier height of the gate metal on the insulator, the GaAs PHEMT reaches a higher value of $BV_{\rm off}$. As both devices are turned on, however, the erosion of $BV_{\rm on}$ in the InP HEMT is significantly more severe than in the GaAs PHEMT.

The fact that impact ionization has a negative temperature coefficient in low-InAs composition InGaAs channels further favors GaAs PHEMT's for high operating temperatures, as is typical of power applications. In InP devices, the positive temperature coefficient of impact ionization makes this phenomenon even more prominent as the temperature goes up. This is clearly undesirable from a power perspective.

It has recently been suggested that InP HEMT's suffer from premature burnout [19] and that burnout is associated with impact ionization in the channel [12], [19]. This is evident in the fact that InP HEMT's with different values of sheet carrier concentration are found to burn out at constant I_G regardless of I_D or n_s, as shown in Fig. 14 [12]. This "universal" behavior is observed when the devices are sufficiently above threshold and the gate current is dominated by impact ionization. The

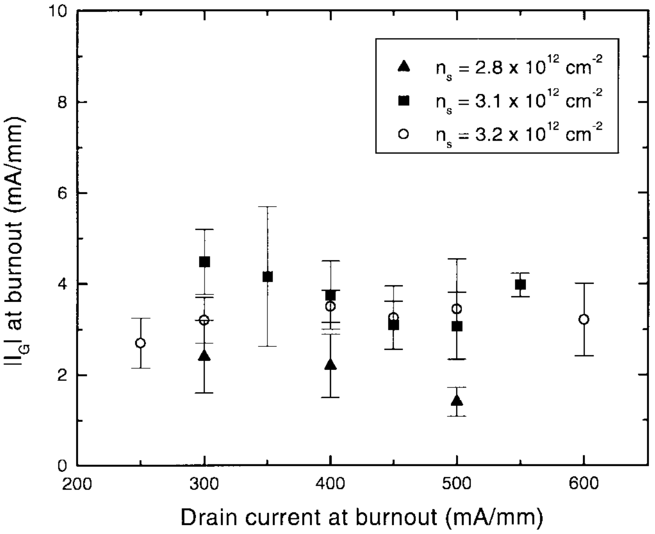

Fig. 14. Gate current versus drain current at burnout for 0.1-μm power InP HEMT's [12].

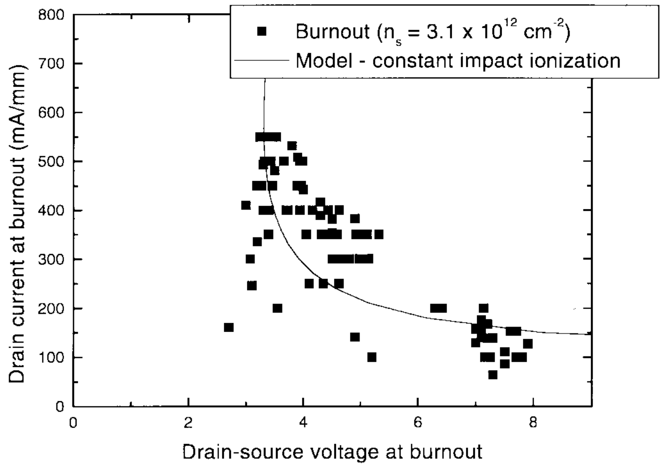

Fig. 15. Comparison of measured burnout points and modeled contour of constant impact ionization in 0.1-μm InP power HEMT's [12].

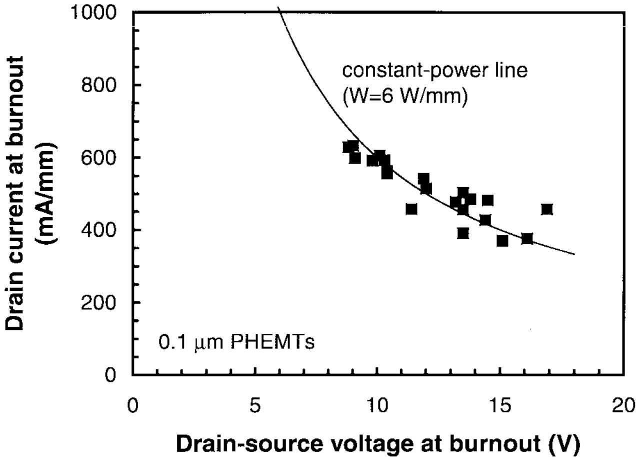

Fig. 16. Comparison of measured burnout points and modeled contour of constant power in 0.1-μm GaAs power PHEMT's [27].

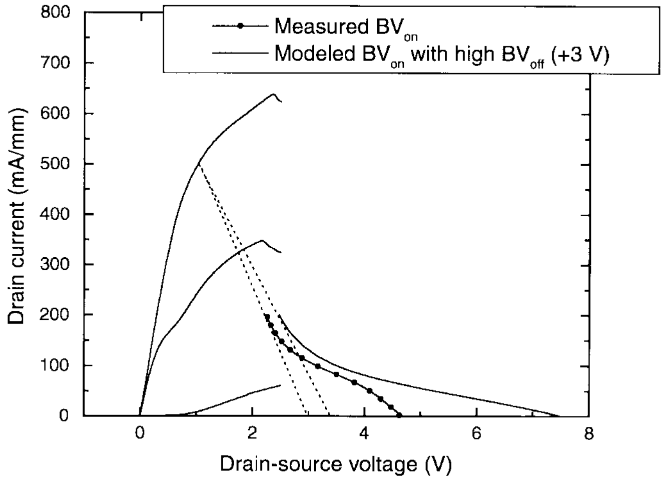

Fig. 17. Modeled change in $BV_{\rm on}$ and maximum power load line of a 0.1-μm power InP HEMT produced by a hypothetical increase in ϕ_B that results in an enhancement of 3 V in $BV_{\rm off}$. The change in the maximum power load line is minor.

burnout locus in the output characteristics also matches a constant impact ionization criteria, as shown in Fig. 15 [12]. This is unlike GaAs PHEMT's in which burnout appears to be of a thermal nature and follows a constant power locus, as graphed for a typical device in Fig. 16 [27]. While this dramatic difference is not yet understood, the higher impact ionization rate of the InAs-rich InGaAs channel and perhaps its positive temperature coefficient might be responsible for it.

IV. OPTIONS FOR BREAKDOWN VOLTAGE IMPROVEMENT IN InP HEMT'S

Improving millimeter-wave power performance of InP HEMT's demands enhancement of their voltage handling capability, that is, increasing $BV_{\rm off}$ and $BV_{\rm on}$. For a given recess design, $BV_{\rm off}$ can only be meaningfully improved by enhancing the Schottky barrier height of the gate. Wide bandgap insulators [28]–[30], alternate gate metals [30], and novel interface treatments [31]–[33] have been explored with limited success. However, the tradeoffs of these schemes in the overall performance of the device are not well documented. In fact, power devices operating above 60 GHz have yet to incorporate any of these new features. Furthermore, the manufacturability of most of these approaches is yet to be demonstrated.

Additionally, improving $BV_{\rm off}$ alone is not enough. Due to the high impact ionization rate in the channel, it is $BV_{\rm on}$ that constitutes the power bottleneck of many device designs. Strategies that enhance $BV_{\rm off}$ do not necessarily improve $BV_{\rm on}$ nor the maximum power. An example is illustrated in Fig. 17, which shows the measured locus of $BV_{\rm on}$ in a typical 0.1-μm power InP HEMT [12]. Also shown in this figure is the change that is to be expected to $BV_{\rm on}$ if $BV_{\rm off}$ could somehow be increased by 3 V without changing anything in the channel of the device (this could be attained, for example, by using a new hypothetical gate metal that yields a higher value of Schottky barrier height). We can reliably make this estimation by means of the models for $BV_{\rm on}$ that were discussed above. As shown, even though the improvement in $BV_{\rm off}$ is substantial, the enhancement in $BV_{\rm on}$ is minimal and the output power would not change significantly. From this, we conclude that it is $BV_{\rm on}$ that constitutes the bottleneck to maximum power in InP power HEMT's.

It should not be concluded from this example, however, that working to improve $BV_{\rm off}$ is altogether irrelevant. Fig. 17 in fact suggests that if a maximum *power-added efficiency* load line (which is shallower than the maximum power load line depicted in Fig. 17) is used, the impact of improving $BV_{\rm off}$ on the power output of the device could be significant. This matters because, as stated in the introduction, the uniqueness of InP HEMT technology in the millimeter-wave regime is its high PAE. Shallower load lines than the ones suggested in Fig. 17 are likely to be used in many applications.

Nevertheless, for InP HEMT's, significant improvements in power density can only be obtained by adequate management of impact ionization. Composite channels [34], [35], compositionally graded channels [36], and quantized channels [35] have all been investigated toward this goal, although long-lasting benefit has not been obtained beyond 60 GHz. Cap recess engineering should also be an effective approach for improving $BV_{\rm on}$. Experiments indicate, for example, that an asymmetric recess should enhance the breakdown voltage and largely preserve the gain [37], as should double recess designs [38]. Although physical understanding is still insufficient, a potential avenue to improve $BV_{\rm on}$ might be the effective draining of impact-ionization generated holes by means of a p-type body contact on the source side of the device [39]. If similarity between the kink effect in InP HEMT's and silicon-on-insulator (SOI) MOSFET's can serve as a guide, the draining of impact ionized holes should result in a suppression of the kink effect and a significant improvement in $BV_{\rm on}$.

V. CONCLUSION

The power potential of InP HEMT's, relative to GaAs PHEMT's, is hampered by their relatively small breakdown voltages. In comparison with GaAs PHEMT's, InP HEMT's are characterized by a small gate Schottky barrier height. This results in a reduced off-state breakdown voltage. Additionally, InP HEMT's suffer from an enhanced impact ionization rate in the channel, yielding a small on-state breakdown voltage. Perhaps more important, the impact ionization rate of InP HEMT's has a positive thermal coefficient. Future improvements in the breakdown voltage of InP HEMT's will require careful management of impact ionization in the channel.

ACKNOWLEDGMENT

The authors are particularly indebted to R. Blanchard, P. C. Chao, G. Duh, T. Enoki, K. Hur, Y. Ishii, H. Rohdin, P. Saunier, P. Smith, and A. Swanson for many enriching discussions.

REFERENCES

[1] Y. C. Chen, D. L. Ingram, R. Lai, M. Barsky, R. Grunbacher, T. Block, H. C. Yen, and D. C. Streit, "A 95-GHz InP HEMT MMIC amplifier with 427-mW power output," *IEEE Microwave Guided Wave Lett.*, vol. 8, no. 11, pp. 399–401, 1998.

[2] H. Wang, Y. Hwang, T. H. Chen, M. Biedenbender, D. C Streit, D. C. W. Lo, G. S. Dow, and B. R. Allen, "A W-band monolithic 175-mW power amplifier," in *Proc. IEEE Microwave Theory Technology Symp.*, 1995, pp. 419–422.

[3] P.-P. Huang, T.-W. Huang, H. Wang, E. W. Lin, Y. Shu, G. S. Dow, R. Lai, M. Biedenbender, and J. H. Elliott, "A 94-GHz 0.35-W power amplifier module," *IEEE Trans. Microwave Theory Technol.*, vol. 45, no. 12, pp. 2418–2423, 1997.

[4] M. Yu, M. Matloubian, P. Petre, L. Hamilton, R. Bowen, M. Liu, H. C. Sun, C. Ngo, and P. Janke, "W-band InP-based HEMT MMIC power amplifiers using finite-ground CPW design," in *Proc. IEEE GaAs Int. Circuit Symp.*, 1998, pp. 37–40.

[5] S. Piotrowicz, C. Gaquiere, B. Bonte, E. Bourcier, D. Theron, X. Wallart, and Y. Crosnier, "Best combination between power density, efficiency, and gain at V-band with an InP-based PHEMT structure," *IEEE Microwave Guided Wave Lett.*, vol. 8, no. 1, pp. 10–12, 1998.

[6] P. M. Smith, S.-M. J. Liu, M.-Y. Kao, P. Ho, S. C. Wang, K. H. G. Duh, S. T. Fu, and P. C. Chao, "W-band high efficiency InP-based power HEMT with 600 GHz $f_{\max}$," *IEEE Microwave Guided Wave Lett.*, vol. 5, no. 7, pp. 230–232, 1995.

[7] O. S. A. Tang, K. H. G. Duh, S. M. J. Liu, P. M. Smith, W. F. Kopp, T. J. Rogers, and D. J. Pritchard, "A 560 mW, 21% power-added efficiency V-band MMIC power amplifier," in *Proc. IEEE GaAs Int. Circuit Symp.*, 1996, pp. 115–118.

[8] P. Greiling and N. Ho, "Commercial satellite applications for heterojunction microelectronics technology," *IEEE Trans. Microwave. Theory Technol.*, vol. 46, no. 6, pp. 734–736, 1998.

[9] J. Dickmann and M. Berg, "InP-based devices and integrated circuits for millimeter-wave sensor and communication systems," in *Proc. Int. Conf. InP and Related Materials*, 1998, pp. 411–414.

[10] K.-F. Lau, L. Liu, and S. Dow, "Recent MMW technology development and its military and commercial applications," in *Proc. IEEE Radio Frequency Int. Circuits Symp.*, 1998, pp. 87–90.

[11] S. Bahl and J. A. del Alamo, "A new drain-current injection technique for the measurement of off-state breakdown voltage in FET's," *IEEE Trans. Electron Devices*, vol. 40, no. 8, pp. 1558–1560, 1993.

[12] M. H. Somerville, R. Blanchard, J. A. del Alamo, G. Duh, and P. C. Chao, "On-state breakdown in power HEMTs: Measurements and modeling," in *Proc. Int. Electron Devices Meeting*, 1997, pp. 553–556.

[13] M. H. Somerville R. Blanchard, J. A. del Alamo, G. Duh, and P. C. Chao, "A new gate current extraction technique for measurement of on-state breakdown voltage in HEMT's," *IEEE Electron Device Lett.*, vol. 19, no. 11, pp. 405–407, 1998.

[14] S. R. Bahl, J. A. del Alamo, J. Dickmann, and S. Schildberg, "Off-state breakdown in InAlAs/InGaAs MODFET's," *IEEE Trans. Electron Devices*, vol. 42, no. 1, pp. 15–22, 1995.

[15] J. Dickmann, S. Schildberg, K. Riepe, B. E. Maile, A. Schurr, A. Geyer, and P. Narozny, "Breakdown mechanisms in pseudomorphic InAlAs/$\rm In_xGa_{1-x}As$ high electron mobility transistors on InP. I: Off-state," *Jpn. J. Appl. Phys.*, vol. 34, pt. 1, no. 1, pp. 66–71, 1995.

[16] K. W. Eisenbeiser, J. R. East, and G. I. Haddad, "Theoretical analysis of the breakdown voltage in pseudomorphic HFET's," *IEEE Trans. Electron Devices*, vol. 43, no. 11, pp. 1778–1787, 1996.

[17] G. Meneghesso, A. Mion, A. Neviani, M. Matloubian, J. Brown, M. Hafizi, T. Liu, C. Canali, M. Pavesi, M. Manfredi, and E. Zanoni, "Effects of channel quantization and temperature on off-state and on-state breakdown in composite channel and conventional InP-based HEMT's," in *Proc. Int. Electron Devices Meeting*, 1996, pp. 43–46.

[18] M. H. Somerville and J. A. del Alamo, "A model for tunneling-limited breakdown in high-power HEMT's," *Proc. Int. Electron Devices Meeting*, 1996, pp. 35–38.

[19] H. Rohdin, C.-Y. Su, N. Moll, A. Wakita, A. Nagy, V. Robbins, and M. Kauffman, "Semi-analytical analysis for optimization of 0.1 μm InGaAs-channel MODFET's with emphasis on on-state breakdown and reliability," in *Proc. Int. Conf. InP and Related Materials*, 1997, pp. 357–360.

[20] A. Neviani, G. Meneghesso, E. Zanoni, M. Hafizi, and C. Canali, "Positive temperature dependence of the electron impact ionization coefficient in $\rm In_{0.53}Ga_{0.47}As$/InP HBT's," *IEEE Electron Device Lett.*, vol. 18, no. 12, pp. 619–621, 1997.

[21] C. S. Putnam, M. H. Somerville, J. A. del Alamo, P. C. Chao, and K. G. Duh, "Temperature dependence of breakdown voltage in InAlAs/InGaAs HEMTs: Theory and experiments," in *Proc. Int. Conf. InP and Related Materials*, 1997, pp. 197–200.

[22] M. H. Somerville, "Limiting physics of millimeter-wave InP power high-electron mobility transistors," Ph.D. dissertation, Massachusetts Institute of Technology, Cambridge, 1998.

[23] M. H. Somerville, J. A. del Alamo, and P. Saunier, "Off-state breakdown in power PHEMTs: The impact of the source," *IEEE Trans. Electron Devices*, vol. 45, no. 9, pp. 1883–1889, 1998.

[24] W. Monch, "Schottky contacts on ternary compound semiconductors: Compositional variations of barrier height," *Appl. Phys. Lett.*, vol. 67, no. 15, pp. 2209–2211, 1995.

[25] S. R. Bahl and J. A. del Alamo, "An $In_{0.52}Al_{0.48}As/n^+$-$In_xGa_{1-x}As$ heterostructure field-effect transistor with an in-enriched channel," in *Proc. Int. Conf. InP and Related Materials*, 1990, pp. 100–103.

[26] L. D. Nguyen, A. S. Brown, M. A. Thompson, L. M. Jelloian, L. E. Larson, and M. Matloubian, "650 Å self-aligned-gate pseudomorphic $Al_{0.48}In_{0.52}As/Ga_{0.20}In_{0.80}As$ high electron mobility transistors," *IEEE Electron Device Lett.*, vol. 13, no. 3, pp. 143–145, 1992.

[27] H. Rohdin and L. Studebaker (HP), private communication, 1998.

[28] S. R. Bahl, W. J. Azzam, and J. A. del Alamo, "Strained-insulator $In_xAl_{1-x}As/n^+$-$In_{0.53}Ga_{0.47}As$ heterostructure field-effect transistors," *IEEE Trans. Electron Devices*, vol. 38, no. 9, pp. 1986–1992, 1991.

[29] M. Matloubian, D. Docter, C. Nguyen, T. Liu, S. Bui, and C. Ngo, "$Ga_{0.47}In_{0.53}As$/InP HEMT's with novel $GaP_{0.35}Sb_{0.65}$ Schottky layers grown by MOVPE," in *Proc. IEEE Dev. Research Conf.*, 1998, pp. 32–33.

[30] M. Amano, S. Fujita, S. Hosoi, T. Noda, A. Sasaki, and Y. Ashizawa, "InAlAs/InGaAs HEMT using InGaP Schottky contact layer," in *Proc. Int. Conf. InP and Related Materials*, 1995, pp. 416–419.

[31] K. Vaccaro, S. M. Spaziani, A. Davis, H. M. Dauplaise, E. A. Martin, and J. P. Lorenzo, "Cadmium sulfide surface stabilization and Schottky barrier enhancement for InP based optoelectronic devices," in *Proc. Int. Conf. InP and Related Materials*, 1995, pp. 817–820.

[32] H. Hasegawa, "Controlled formation of high Schottky barriers on InP and related materials," in *Proc. Int. Conf. InP and Related Materials*, 1998, pp. 451–454.

[33] S. Habibi, M. Totsuka, J. Tanaka, and S. Matsumoto, "Improvement in Schottky diode characteristics of metal-InAlAs contact using an in situ photochemical etching and surface passivation process," in *Proc. Int. Conf. on InP and Rel. Mat.*, 1995, pp. 821–824.

[34] P. Chevalier, X. Wallart, F. Mollot, B. Bonte, and R. Fauquembergue, "Composite channel HEMT's for millimeter-wave power applications," in *Proc. Int. Conf. InP and Related Materials*, 1998, pp. 207–210.

[35] G. Meneghesso, A. Neviani, R. Oesterholt, M. Matloubian, T. Liu, J. J. Brown, C. Canali, and E. Zanoni, "On-state and off-state breakdown in GaInAs/InP composite-channel HEMT's with variable GaInAs channel thickness," *IEEE Trans. Electron Devices* vol. 46, no. 1, pp. 2–9, 1999.

[36] M. Wojtowicz, R. Lai, D. C. Streit, G. I. Ng, T. R. Block, K. L. Tan, P. H. Liu, A. K. Freudenthal, and R. M. Dia, "0.10 μm graded InGaAs channel InP HEMT with 305 GHz f_T and 340 GHz $f_{\max}$," *IEEE Electron Device Lett.*, vol. 15, no. 11, pp. 477–479, 1994.

[37] D. G. Ballegeer, I. Adesida, C. Caneau, and R. Baht, "Physics and behavior of asymmetrically recessed InP-based MODFET's fabricated with an electron beam resist process," in *Proc. Int. Conf. InP and Related Materials*, 1994, pp. 331–334.

[38] K. Y. Hur, R. A. McTaggart, B. W. LeBlanc, W. E. Hoke, P. J. Lemonias, A. B. Miller, T. E. Kazior, and L. M. Aucoin, "Double recessed AlInAs/GaInAs/InP HEMT's with high breakdown voltages," in *Proc. GaAs IC Symp.*, 1995, pp. 101–104.

[39] T. Suemitsu, T. Enoki, and Y. Ishii, "Body contacts in InP-based InAlAs/InGaAs HEMT's and their effects on breakdown voltage and kink suppression," *Electron Lett.*, vol. 31, no. 9, pp. 758–759, 1995.

J. A. del Alamo received the Telecommunications Engineer degree from the Polytechnic University of Madrid, Spain, in 1980 and the M.S. and Ph.D. degrees in electrical engineering from Stanford University, Stanford, CA, in 1983 and 1985, respectively.

From 1977 to 1981, he was with the Institute of Solar Energy of the Polytechnic University of Madrid working on silicon solar cells. At Stanford University, he carried out his Ph.D. dissertation on minority carrier transport in heavily doped silicon. From 1985 to 1988, he was a Research Engineer with NTT LSI Laboratories in Atsugi, Japan, where he conducted research on heterostructure field-effect transistors based on InP, InAlAs, and InGaAs. Since 1988, he has been with the Department of Electrical Engineering and Computer Science, Massachusetts Institute of Technology (MIT), Cambridge, where he is currently a Professor. His current research interests are in gigahertz power transistors: Si LDMOS on SOI, GaAs PHEMT's, and InP HEMT's.

From 1991 to 1996, Prof. del Alamo was an NSF Presidential Young Investigator. In 1992, he received the Baker Memorial Award for Excellence in Undergraduate Teaching at MIT. In 1993, he received the H. E. Edgerton Junior Faculty Achievement Award at MIT.

M. H. Somerville received the B.S. degree in electrical engineering and the B.A. degree in liberal arts from the University of Texas at Austin in 1990, the B.A. degree in physics from Oxford University, U.K., in 1992, and the M.S. and Ph.D. degrees in electrical engineering from the Massachusetts Institute of Technology (MIT), Cambridge, in 1993 and 1998, respectively.

In 1998, he joined the Department of Physics and Astronomy, Vassar College, Poughkeepsie, NY, as an Assistant Professor. From 1989 to 1990, he was a Systems Engineer at SEMATECH, where he worked on the development of modular automation approaches for semiconductor manufacturing. During this time, he also worked at the University of Texas on Monte Carlo simulation of InAlAs/InGaAs HBT's. At MIT, he conducted research on charge control and transport heavily doped quantum wells from 1992 to 1993. His doctoral research focused on fabrication, modeling, and characterization of InAlAs/InGaAs HEMT's for power applications.